applied sciences

MDPI

Article

Fluorescence Masking Based Multifunctional Quantum Dots' Assay for HSP90α Interactions Detection

Anusha Kishore [1], Lu Fan [1], Frank Stahl [2], Thomas Reichel [3], Karsten Krüger [3] and Carsten Zeilinger [1,*]

[1] Centre of Biomolecular Drug Research, (BMWZ), Leibniz University Hannover, 30167 Hannover, Germany
[2] Institute of Technical Chemistry, Leibniz University Hannover, 30167 Hannover, Germany
[3] Department of Exercise Physiology and Sports Therapy, Institute of Sports Science, Justus-Liebig University Giessen, 35394 Giessen, Germany
* Correspondence: zeilinger@cell.uni-hannover.de; Tel.: +49-511-762-16351

Featured Application: The quantum dots-based assay described here uses fluorescence masking to detect protein–ligand and protein–protein interactions on a glass slide in a multifunctional way. This is used here for the stress protein HSP90α in purified form and in cell lysate. It can be further used for other different proteins.

Abstract: HSP90α is one of the most common stress proteins in cells; hence, it is a good target for developing drugs and testing systems for cancer or physical stress levels in humans. Streptavidin conjugated quantum dots (Sav-QDs) are widely used as fluorophores for biosensing to overcome chemical labelling problems. In this work, we have attempted to develop a multifunctional and robust assay for HSP90α. The detection technique was based on the masking of the fluorescence of spotted Sav-QDs on nitrocellulose chips (NC). Biotinylated ligand/antibody attaches to the spotted Sav-QD and then HSP90α is attached, which causes the masking of fluorescence. The masking of fluorescence was used to detect protein–ligand interactions, the effect of inhibitors, protein–protein interactions, and the presence of protein in the biological sample. The load of detection (LoD) of the assay lies in the nano molar range, making it a sensitive assay. The results from the experiments suggest that the used approach is promising for developing a multifunctional, robust, and sensitive assay for proteins that can be used for point-of-care detection in complex biological samples.

Keywords: quantum dots; Sav-QD; biotin-ATP; biotin-HSP90 antibody; HSP90α; fluorescence masking

Citation: Kishore, A.; Fan, L.; Stahl, F.; Reichel, T.; Krüger, K.; Zeilinger, C. Fluorescence Masking Based Multifunctional Quantum Dots' Assay for HSP90α Interactions Detection. *Appl. Sci.* **2023**, *13*, 2957. https://doi.org/10.3390/app13052957

Academic Editor: Yurii K. Gun'ko

Received: 16 December 2022
Revised: 8 February 2023
Accepted: 22 February 2023
Published: 25 February 2023

1. Introduction

Heat shock proteins (HSPs) are highly conserved and the most abundant molecular chaperones in eukaryotes and prokaryotes [1]. The heat shock response was initially observed as puffs in fly chromosomes induced by heat, which was characterized by the fast induction of limited subsets of proteins [2]. HSPs as molecular chaperones facilitate the folding or unfolding of secondary structures of proteins during cellular stress. One of the most abundant molecular chaperones in eukaryotes is HSP90. It is a homodimer, and each unit contains three flexible regions: an N terminal binding domain (NTD), a middle domain, and a C terminal dimerization domain (CTD) [3]. HSP90 is overexpressed in cancer cells. Intensive research is being conducted for searching small molecular inhibitors for HSP90 as anticancer therapeutics [4]. HSP90 has a weak ATPase activity, with a turnover rate of 0.1 min^{-1}. There are two groups of natural product inhibitors for HSP90 based on geldanamycin and radicicol. They bind to the NTD region and inhibit the interaction with ATP, thus stopping the chaperone activity. The K_d value of HSP90α and radicicol is around 0.4 nM [5]. Various internal and external physiological and mechanical stress factors induce a homeostatic imbalance, causing the increased expression of HSP70 and 90 [6]. HSPs

play a role in the pathogenesis, prognosis, and treatment of various diseases. Due to their cytoprotective function, intracellular HSPs are induced as a result of stress. It is suggested that extracellular HSPs are released from damaged cells and their presence has a regulatory function [7]. Various assays have been developed using isothermal titration calorimetry, ligand immobilization, FRET, and fluorescent polarization to monitor the HSP90 concentration and as well as its interaction with inhibitors. These methods require a high protein concentration or a chemical modification of the ligand. Hence, it is very important to develop a convenient, rapid, and robust assay that can detect HSP90 interaction with small molecules, antibodies, and their presence in biological samples [8,9].

Transferring emerging nanotechnologies to the field of biology and medicine has led to the widespread usage of quantum dots (QDs). They are a novel class of multifunctional inorganic fluorophores [10–12]. There are many kinds of QDs available in the market for bioimaging, such as carbon (CQD), graphene (GQD), and semiconductor QDs. GQDs are derived from graphene or graphene oxides, and they are subsets of CQDs. They have a lower toxicity and biocompatibility compared to semiconducting QDs. Their major drawbacks are a lower lifetime and low quantum yield, leading to decreased brightness [13,14]. Semiconducting QDs have a nanocrystal core of groups II–IV or III–V elements, such as CdSe, CdTe, etc., and ZnS shell [15,16]. These are spherical particles with size-dependable optical properties such as absorbance, photoluminescence, etc., resulting from the quantum confinement effects of electron and hole carriers at a dimension smaller than the Bohr exciton radius (separation distance between the electron and hole in an exciton) [17,18]. Their bandgap energy decreases with an increase in the particle size. Upon excitation with a light source, electrons absorb the energy and jump from the valence band, creating a positively charged hole in the conduction band. This creates electron–hole pair (exciton). The electron recombines immediately with the hole, releasing energy equivalent to the bandgap. It is more likely that trap states within the QDs' material will trap the electron or hole, causing a non-radiative emission. Trap states exist due to defects in the lattice structure of the material. To decrease the trap states, the surface passivation of the core material is achieved by coating it with a wider bandgap semiconductor shell (e.g., the CdSe core is coated with a ZnS shell). This makes QDs more favorable as fluorescent labels [18]. QDs are inherently hydrophobic; they are made water-compatible by surface caping with bifunctional ligands that mediate solubility and attachment sites for the bioconjugation of ligands with a terminal carboxylic acid. Positively charged avidin can interact with negatively charged carboxylic acid, forming a bridge for attaching any biotinylated proteins or ligands [11,19]. Avidin interacts stoichiometrically with biotin, and one biotin binds with one avidin subunit. This high-affinity interaction ($K_d = 10^{-15}$ M) is exploited for bioimaging and biosensors using biotinylated nucleic acids and proteins [20]. This technique can be used for any type of nanoparticle regardless of the materials' properties [21]. Common organic dyes such as cyanine (Cy5 or Cy3) that have a resonant emission are called resonant dyes. The emission in them originates from the optical transitions of electrons delocalized over whole chromophore. These dyes have narrow absorption and emission bands that often mirror each other. This poor separation often causes crosstalk between different dye molecules. They also have a small stroke shift and moderate-to-high quantum yield [22]. In contrast to these dyes, QDs have a broad excitation/absorption band ranging from UV to visible light so that a single wavelength can excite different-sized QDs. They have a narrow emission band, which is related to the QDs' nanocrystal radius and core material; it is highly suitable for multiplexing applications. QDs have a high fluorescence quantum yield in the visible range and high molar coefficients. In addition, CdSe-ZnS QDs have an exceptional resistance to photodegradation, and heat compared to organic fluorophores [18]. The binding of organic dyes to biomolecules can disrupt the binding affinity of proteins and ligands. Additionally, the binding of proteins to QDs suffers from site-specific and steric hinderance problems. The conjugation of Sav-QDs with biotinylated antibodies or antigens with nanoparticles will increase the physiochemical stability and provide a target-specific probe character to the QD–antibody/antigen complex [18,23].

Conventional laboratory assays such as an ELISA, RT-PCR, and nucleic acid sequence-based amplification (NASBA) require highly skilled operators, complex procedures, and fancy equipment [24]. A contactless inkjet printer is a low-cost and high-performance method for the printing of biomaterials, based on the ejection of drops from the nozzle in a picolitre volume controlled by piezoelectric micro pumps. This is used for making highly miniaturized, rapid, and robust assays [24,25].

The current work aims to develop a miniaturized and multifunctional assay system based on the masking of Sav-QDs' fluorescence. The assay is used for detecting the presence of the stress protein (HSP90α), a protein–ligand interaction, and the effect of the inhibitor [26]. This is achieved by the interaction of a biotinylated antibody or ligand with HSP90α (Scheme 1). The fluorescence masking results are quantitatively analyzed by a dose–response curve and Stern–Volmer plot. The method is fast, simple, and convenient, with a potential point-of-care application.

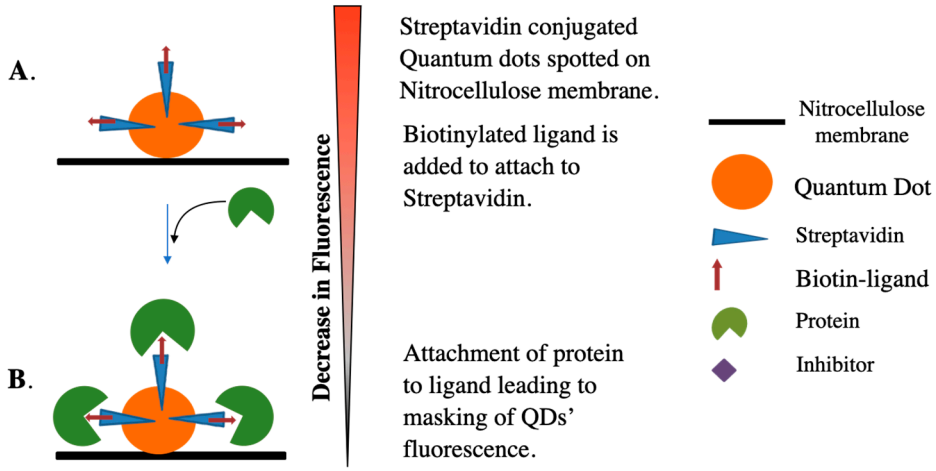

Scheme 1. Schematic overview of a highly miniaturized QD sensor for flexible applications. (**A**) Sav-QD solution was spotted on the nitrocellulose membrane using the contactless printer. Attachment of biotin–ligand to streptavidin molecules, which was transferred to the chip in solution. (**B**) Attachment of protein molecules to biotin–ligand and causing fluorescence masking of Sav-QDs.

2. Materials and Methods

2.1. Reagents and Instrumentation

Spotting was conducted using a contactless microarray printer (Nano-Plotter 2.1) from GeSim (Radeberg, Germany). The scanning of the slides was performed by a microarray scanner from (GenePix 4000B) from Molecular Devices, Axon instruments (San Jose, CA, USA). The fluorescence of the Sav-QD, antibody, and HSP90α mixture was measured using a fluorescence microscope, i.e., a Cytation 5 imaging reader from BioTek (Bad Friedrichshall, Germany).

Sav-QD, which was CdSe-ZnS QDs (Qdots 655), was purchased from Thermofisher (Darmstadt, Germany), and NC-coated glass slides were received from Sartorius (Göttingen, Germany). Radicicol was purchased from Biomol (Hamburg, Germany), Cy5-ATP was obtained from Jena Bioscience (Jena, Germany), biotin-ATP was from Carl Roth (Karlsruhe, Germany), biotin-Anti HSP90 (biotin rabbit polyclonal to HSP90, ab79649) was received from Abcam (Amsterdam, The Netherlands), and blocking buffer was the blocking solution from Candor (Wangen, Germany). The Anti HSP90 primary antibody (SMC-147) was received from StressMarq Biosciences Inc. (Victoria, Canada) and the anti-mouse alkaline phosphatase secondary antibody (A1047) was from Sigma-Aldrich (Taufkirchen, Germany).

Then, 10× FP1 buffer was made by mixing 20 mM of Hepes, 50 mM of KCl, 5 mM of MgCl2.6H2O, 0.01% Tween 20, and 0.1 mg/mL BSA. The 1× FP1 buffer (pH 7.3) was made by adding 1 mM of DTT, 2% v/v DMSO, and 20 mM of $Na_2MoO_4.2H_2O$; the buffer was

stored at 4 °C. PBS buffer (137 mM of NaCl, 2.7 mM of KCl, 10 mM of Na_2HPO_4, 1.8 mM of KH_2PO_4, pH 7.4) was prepared by mixing the solution of NaCl, Na_2HPO_4, and NaH_2PO_4.

Human HSP90α (stock concentration 3 mg/mL or 33 μM) was recombinantly synthesized in *E. coli* BL21DE3 cells and purified as described by Schax et al. [27].A microarray-based Cy5-ATP and radicicol sensitive binding assay was performed to determine the ATP-binding activity described by Yue et al. [19]. Murine fibroblasts (NIH3T3, ATCC® CRL-1658TM) and human cervix epithelial cells (Hela, ATCC CCL-2) were cultured in DMEM (Dulbecco's Modified Eagle Medium, Bio&Sell BS. FG 0445) containing 10% FCS (Bio&Sell BS. L 2045) and 1% penicillin–streptomycin mix (Bio&Sell BS-AB17.07001) in a humidified environment with 5% CO_2 at 37 °C. The culture was then harvested when confluency reached nearly 100% by trypsin (0.02% EDTA included) and pelleted at 3000 rpm for 10 min after washing with Hank's Buffered Salt Solution (Bio&SELL BS. L 2045). The cells were subsequently disrupted by adding glass beads and sonicated in buffer (20 mM of Tris-HCl pH 8.0, 500 mM of KCl, 2 mM of β-mercaptoethanol, 2 mM of imidazole, 10% glycerin, 1% protease inhibitor cocktail (Carl Roth 3751.1), 10 mM of dithiothreitol) for 10 s and 6 times on the ice. The lysates were centrifugated at a speed of 17,000× *g* for 10 min at 4 °C. The supernatant was then subject to dialysis overnight in PBS buffer.

All solutions were made using double distilled water and analytical grade reagents. Overnight incubation of the chips was carried out at 4 °C, with slow shaking and dark conditions. The scanning of the slides was performed with a 635 nm laser, 350 PMT gain, and 33% power. The excitation wavelength, emission wavelength, and gain were set to 500 nm, 655 nm, and 100 for the fluorescence microscopy measurements.

2.2. Fabrication of Sav-QDs Assays

Columns containing ten spots of Sav-QDs were spotted in concentrations of 10, 20, 40, 50, 60, 80, and 100 nM solutions diluted in 1× FP1 buffer. Spotting was done using the nano-plotter on an NC slide. The slide was dried with compressed air at room temperature; the slide was then scanned. Afterwards, a slide was fixed in the incubation chamber having sixteen blocks for NC pads on the slide (eight rows and two columns). To each pad, 100 μL of the blocking buffer was added. The chamber was covered with PCR slips and aluminum foil. Incubation was carried out for 1h on a shaker at room temperature. The buffer was discarded, and the slide was removed from the incubation chamber. It was completely dried with compressed air. The slide was scanned again to check the adherence of the Sav-QDs and the estimation of the optimal Sav-QDs concentration range for later measurements.

2.3. Testing Protein–Ligand Interaction with and without Inhibitor

2.3.1. With Biotinylated ATP

Columns of ten spots of 100 nM of Sav-QDs were spotted and blocked. Next, 50 μL of biotin-ATP of different concentrations (1, 5, 10, 50, 100, 500, 1000, and 5000 nM) diluted with 1× FP1 buffer was added to each pad on the slide followed by 45 min incubation in ice and on a shaker. Biotin-ATP was discarded, and the slide was dried with compressed air. The slide was incubated overnight with purified human HSP90α with the same concentrations as biotin-ATP. HSP90α was discarded and the slide was dried with compressed air. Scanning was done to check the masking of the fluorescence after incubation with HSP90α.

2.3.2. With Radicicol and Biotinylated ATP

In total, 1 μM of radicicol completely inhibits the binding of 100 nM of Cy5-ATP to 33 μM of HSP90α, as seen in Figure 1. As mentioned above, 10 spots of 100 nM of Sav-QDs were spotted on the microarray slide, blocked, and incubated with constant concentrations of biotin-ATP (500 nM), which was incubated with varying concentrations of HSP90α (0.05, 0.5, 5, 50, 500, and 5000 nM) and 1 μM of radicicol. The experiment was repeated with varying concentrations of the mixture of HSP90α and streptavidin and a constant concentration of the inhibitor. The mixture was made by mixing and the

overnight incubation of HSP90α (5, 10, 50, 100, 500, and 1000 nM) and 1μM of radicicol and streptavidin. For each HSP90α concentration, the streptavidin concentration was ten times more.

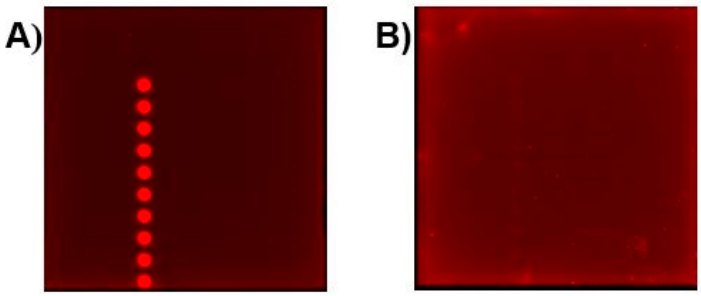

Figure 1. (**A**) Spotted and blocked HSP90α with attached Cy5-ATP. (**B**) In the presence of 1 μM radicicol, there is incomplete inhibition of binding of Cy5-ATP. Schematic overview of a highly miniaturized QD sensor for flexible applications.

2.4. Testing Protein–Protein Interaction

2.4.1. Checking Sensitivity of the Assay

Similar to the previous assay, biotin-Hsp90 antibody (0.01, 0.05, 0.1, 0.5, 1, 5, 10, 50, 100, and 500 nM) was used instead of biotin-ATP. To each pad with 10 spots of 50 nM of Sav-QDs which were blocked, 50 μL of biotin antibody of different concentrations diluted in PBS buffer was added, followed by a 45 min incubation on ice and in a shaker. The biotin antibody was discarded, and the slide was dried with compressed air. Overnight incubation with Hsp90α was conducted. The concentration in each pad was the same as the concentration of biotin antibody. Hsp90α was discarded, and final the slide was scanned to check the masking effect.

To decipher the sensitivity, the load of detection (LoD) and load of quantitation (LoQ) Stern–Volmer graph was plotted with the magnitude of quenching (F0/F) versus the HSP90α concentration ranging from 100 to 1 nM. F0 and F are the fluorescence intensities of Sav-QDs after adding the antibody and HSP90α, respectively. For each concentration, a mean value of five spots was taken. As the magnitude of fluorescence quenching is linearly proportional to the HSP90α concentration, the Stern–Volmer equation was applied.

2.4.2. Confirming the Binding of Protein to Biotinylated Antibodies Attached to Sav-QDs

To confirm the binding and function of the biotin-HSP90 antibody to HSP90α, the fluorescence was measured in solution using a fluorescence microscope. In total, 50 μL of 50 nM Sav-QD with 100, 50, and 10 nM of biotin-HSP90 antibody solutions were made in PBS buffer and incubated for one hour on a shaker at 4 °C. The fluorescence was measured by transferring the solutions to a 96-well plate without any air bubbles. HSP90α solutions were made by mixing 50 nM of Sav-QD with 100, 50, and 10 nM of biotin-HSP90 antibody and incubating for one hour on the shaker at 4 °C. This was followed by adding HSP90α with the same concentration as the antibody, and the volume was made to 50 μL with PBS buffer. Overnight incubation was carried out, after which the fluorescence was measured.

2.5. Checking Protein in Cell Lysate

2.5.1. Using Sav-QD Assay to Detect HSP90α in Cell Lysate

A total of 50 nM of Sav-QDs were spotted and blocked. Then, 500 nM of biotin-HSP90 antibody was added and incubated for 45 min on ice, in a shaker. The antibody solution was discarded, and the chip was dried with compressed air. Overnight incubation was carried out with HeLa cell lysates. They were used in a stock concentration; there were ten-fold and one hundred-fold diluted concentrations. The cell lysates were discarded; the chip was dried and scanned.

2.5.2. Confirming Presence of HSP90α in Cell Lysate with Western Blot

HSP90α in HeLa cell lysate was analyzed by Western blotting with Anti HSP90 primary antibody and anti-mouse alkaline phosphatase secondary antibody. The stock solution and 10× and 100× diluted solutions of HeLa cell lysate were used in the Western blot. Purified HSP90α was used as a positive control and fibroblast lysate was used as a negative control.

2.5.3. Confirming the Binding of HSP90α in Cell Lysate with Biotin-HSP90 Antibody

HeLa cell lysate solution was made by mixing 50 nM of Sav-QD with 100 nM of biotin-HSP90 antibody and incubating for one hour in a shaker at 4 °C. This was followed by adding HeLa cell lysate stock, and the volume was made to 50 µL with PBS buffer. The cell lysate was 10× times diluted in the solution. Overnight incubation was carried out, after which the fluorescence was measured with the same parameters as used for the antibodies and HSP90α.

3. Results and Discussion

3.1. Human HSP90α Activity

Human HSP90α was recombinantly synthesized, purified, and tested on a microarray-based assay for radicicol sensitive ATP-Cy5 binding, as shown by Yue et al. [19]. Figure 1 shows that 1 µM of radicicol completely displaces the binding of Cy5-ATP. Thus, it was confirmed that HSP90α was active and used for further experiments.

3.2. Sav-QDs Assay

The aim was to establish a quantum dots-based multifunctional and robust assay using HSP90α as a sample protein. That can be further developed into a point-of-care assay for other stress proteins. To check the stability of Sav-QDs and to estimate the optimal concentration range for working, a series of different QD concentrations were spotted on the NC slides, and the signal intensities for each concentration with and without a blocking buffer treatment were measured. The signal intensities were provided as a mean fluorescence of ten spots (Figure 2a). For each concentration of Sav-QDs, the signal mean was subtracted with the background mean and the overall mean value for ten spots was plotted against the concentration. There was a decrease in the fluorescence intensity in a concentration-dependent manner, and the blocking solution had no significant influence on the signal intensity; only a little weakening effect was observed (Figure 2b). A 100–50 nM QD concentration was chosen initially for the masking experiment because of a high fluorescence.

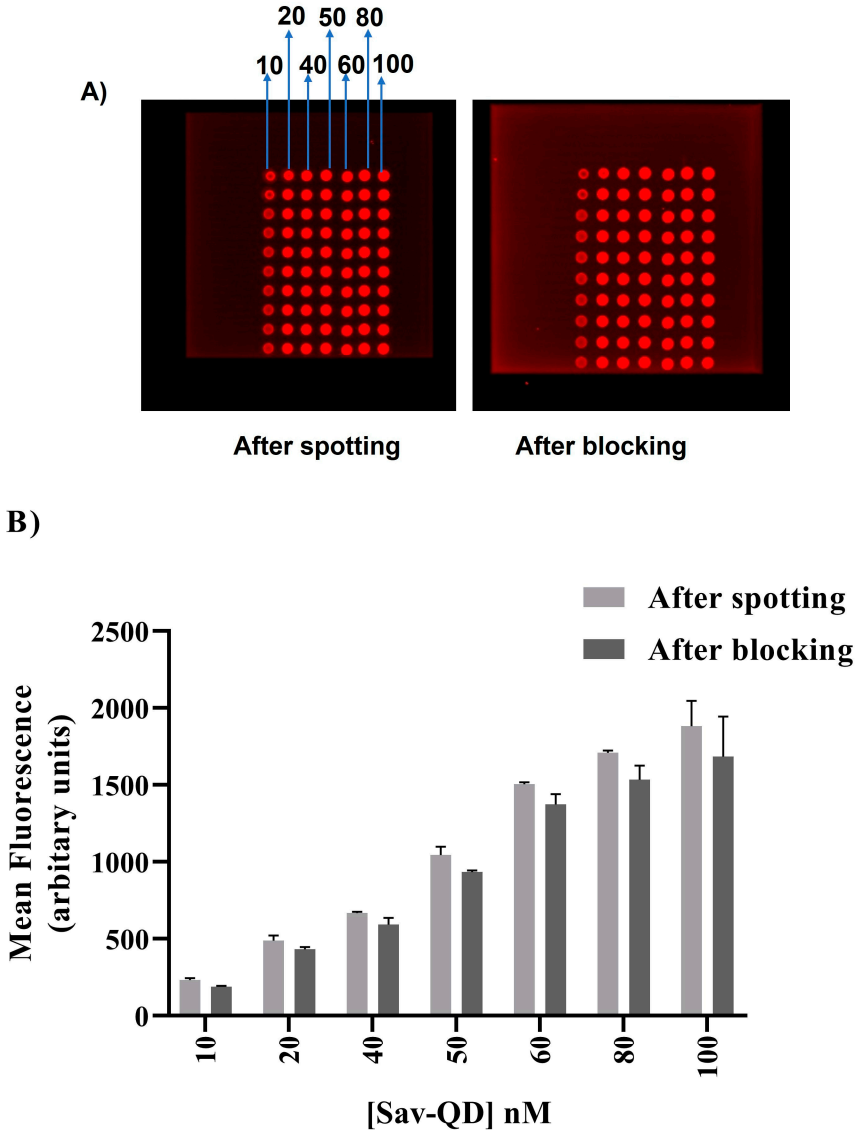

Figure 2. (**A**) Sav-QDs of 10, 20, 40, 50, 60, 80, and 100 nM concentrations which are spotted and blocked. (**B**) The fluorescence intensity of spotted Sav-QDs is concentration-dependent and the blocking buffer does not cause any significant reduction in the signal. The mean fluorescence signal (signal mean–background mean) is plotted against different concentrations of Sav-QDs.

3.3. Testing Protein–Ligand Interaction with and without Inhibitor

3.3.1. With Biotinylated ATP

A 100 nM Sav-QD concentration was chosen initially as it was providing the highest fluorescence. Different concentrations of biotin-ATP were added to the spotted Sav-QDs to form attachment points for HSP90α. The concentrations of 1, 5, 10, 50, 100, 500, 1000, and 5000 nM were chosen because each QD particle has around 5 to 10 streptavidin molecules attached to it (this value is from the company's description of the product). After spotting, 1–5 of the streptavidin molecules will be available for attachment to the biotinylated ligand (biotin-ATP). The rest are unavailable as they are either hidden (assuming that, after spotting, only the top half of the QD sphere is available for binding) or are difficult to access (due to a steric hindrance between the protein molecules that will attach). Hence, 100 nM of ten QD spots correspond to around a 1000 to 5000 nM streptavidin binding capacity on each pad.

The binding of recombinantly synthesized and purified HSP90α via biotinylated ATP to the Sav-QDs led to the masking of its fluorescence in a concentration-dependent manner,

as shown in Figure 3. There was a complete masking from a 500 nM concentration of HSP90α and around 1 nM, there was signal saturation for a lower concentration of HSP90α. Hence, for further experiments, a concentration range of 1–500 nM will be better suited. The concentration-dependent masking of the fluorescence intensity presented an EC_{50} value of 15.2 nM. The sensitivity of the assay lies nearby this value.

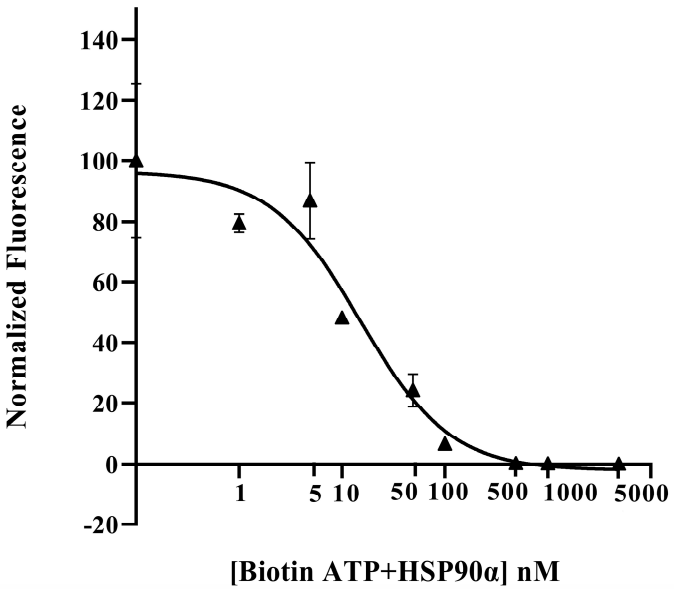

Figure 3. Fluorescence masking of Sav-QDs as a function of biotin-ATP and HSP90α concentration. Concentration-dependent masking is fitted in a dose-responsive manner with an EC_{50} value of 15.20 nM. Maximum fluorescence intensity is counted as 100%, which is only FP1 buffer. The concentration of spotted Sav-QDs was 100 nM. Parameters of the dose–response fitting, A1 = 0 nM, A2 = 5000 nM, slope = −1.12, log X = 1.182, and X = 15.20. Normalized fluorescence is plotted against biotin-ATP and HSP90α concentration.

3.3.2. With Radicicol and Biotinylated ATP

To check the diversified usage of the Sav-QDs assay, i.e., testing compounds as the potential inhibitors of protein–ligand interactions, HSP90α was pre-incubated with 1 µM of radicicol. A small shift in the binding affinity of HSP90α to biotin-ATP attached to spotted Sav-QD was observed with an EC_{50} value of 92.06 nM for the influence of radicicol (Figure 4a). A complete reduction or significant shift in the EC_{50} value by the presence of radicicol was not observed. This can be explained by the non-specific binding of HSP90α. To improve on this, streptavidin was added to the mixture of HSP90α and radicicol to block the hydrophobic pockets on the surface of HSP90α. A significant increase in the EC_{50} value to ~396 nM for the mixture of radicicol, HSP90α, and streptavidin was observed compared with the EC_{50} value of ~52 nM for only HSP90α and streptavidin (Figure 4b). For the complete inhibition of HSP90α binding to biotin-ATP in the presence of radicicol, good filtration and washing steps will be required to remove unbound radicicol and protein. Even with constant biotin-ATP, the masking of fluorescence by HSP90α was in a concentration-dependent manner. This shows that the assay can be used more robustly, and it can be further applied to test new inhibitory compounds.

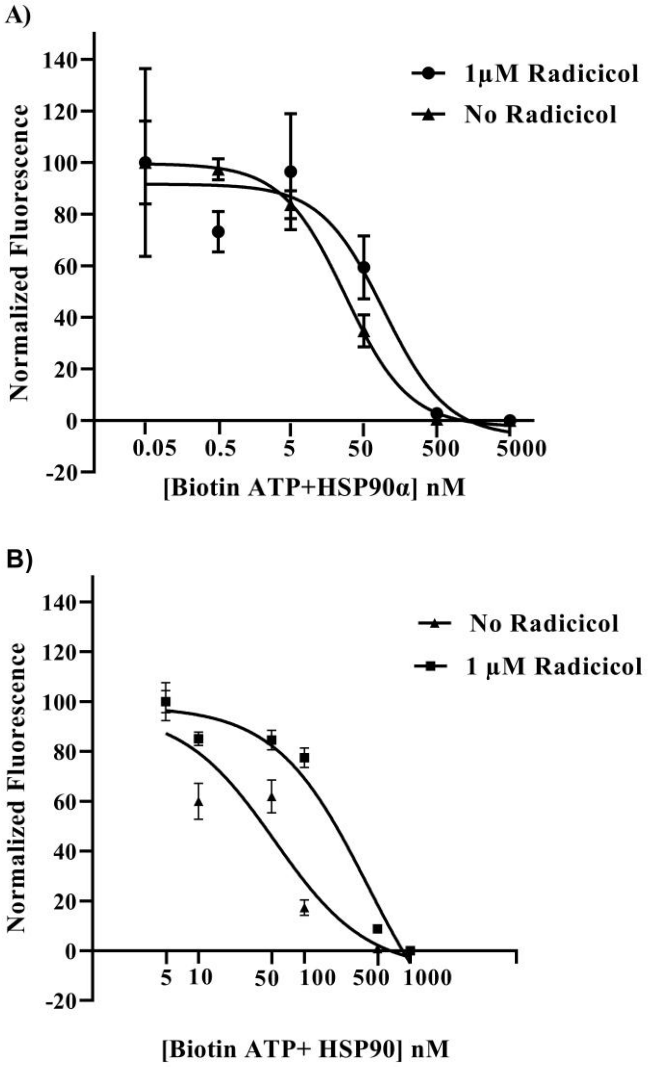

Figure 4. Concentration-dependent masking is fitted in a dose-responsive manner. Maximum fluorescence intensity is counted as 100%, which is 0.05 nM and 5 nM HSP90α in graphs (**A**,**B**), respectively. The concentration of the Sav-QDs was 100 nM. In graph (**A**), masking of Sav-QDs was achieved as a function of biotin-ATP which was kept constant at 500 nM and varying only HSP90α concentration with and without radicicol. IC_{50} value of the graph with 1 μM of radicicol is 92.06 nM and without radicicol is 27.27 nM. Additionally, in graph(**B**), there is a varying Hsp90α concentration with ten times the streptavidin concentration with and without radicicol. IC_{50} values of graphs with radicicol is 396.7 nM and without radicicol is 52.21 nM. Parameters of the dose–response fitting for graph (**A**), A1 = 0.05, A2 = 5000, p = 1 log X = 1.964 (1 μM of radicicol), 1.436 (no radicicol) X = 92.06 (1 μM of radicicol), 27.27 (no radicicol). Parameters of the dose–response fitting for graph (**B**), A1 = 5, A2 = 1000, p = 1 log X = 2.598 (1 μM of radicicol), 1.718 (no radicicol), X = 396.7 (1 μM of radicicol), 52.21 (no radicicol).

3.4. Testing Protein–Protein Interaction

3.4.1. Checking the Sensitivity of the Assay

In Figure 5, it is shown that HSP90α masked the fluorescence intensity of the Sav-QDs by binding on the biotinylated anti HSP90α in a dose-dependent manner and presented an EC_{50} value of ~43 nM. These data thus indicate that Sav-QDs can be used as a microarray-based sensor for detecting the presence of a specific antigen qualitatively and quantitatively.

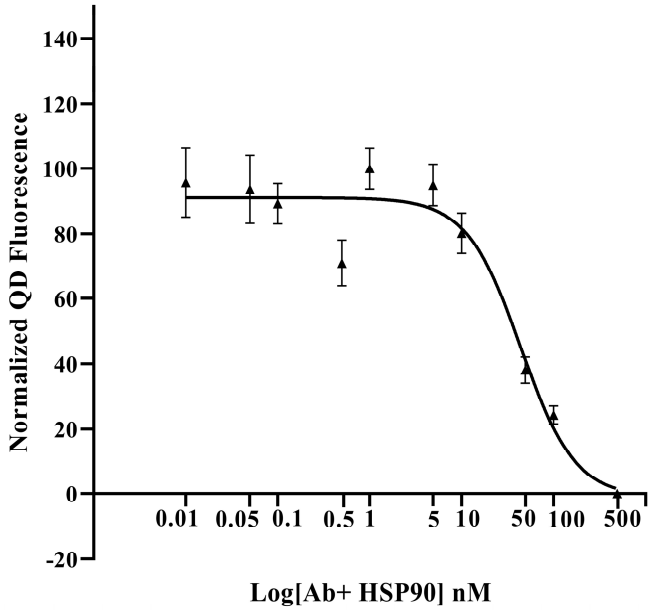

Figure 5. Masking of Sav-QDs as a function of biotin-HSP90 antibody and HSP90α concentration. Concentration-dependent masking fitted in a dose-responsive manner with an EC_{50} value of 43.96 nM. Maximum fluorescence intensity is counted as 100%, which is 0.1 nM of biotin antibody and Hsp90α. Concentration of the Sav-QDs was 50 nM. Parameters of the dose–response fitting, A1 = 00.1 nM, A2 = 500 nM, slope = −1.467, log X = 1.643, X = 43.96.

This was done to calculate the sensitivity, LoD, and LoQ of the assay and further apply the principle to detect HSP90α in complex biological samples such as HeLa cell lysate. Here, 50 nM of Sav-QDs spots were used instead of 100 nM because, in this case, the masking of the fluorescence was not as high as biotin-ATP and Hsp90α. It was assumed that a bigger antibody size was causing steric hindrance, hence not many of them attaching to Sav-QDs as compared to biotin-ATP; in the end, lesser HSP90α binds. A 50 nM concentration of Sav-QDs has a lower fluorescence than 100 nM, providing a better analysis in a concentration-dependent manner for the biotin antibody and HSP90α. To obtain a linear relationship between the protein concentration and fluorescence masking, a concentration range of 1–100 nM was chosen. As it was seen in the dose–response curve (Figure 3) with biotin-ATP and HSP90α, concentrations above 100 nM and below 1 nM were in the saturation range. From the graph, in Figure 6, K_{SV} is evaluated to be 0.06784 nM^{-1} with linear data regression (r^2 = 0.97). The LoD and LoQ of the assay are 5.18 nM (0.45 µg/mL) and 15.2 nM (15.62 µg/mL). These values are nearby the EC_{50} value of the biotin-ATP and HSP90α binding assay.

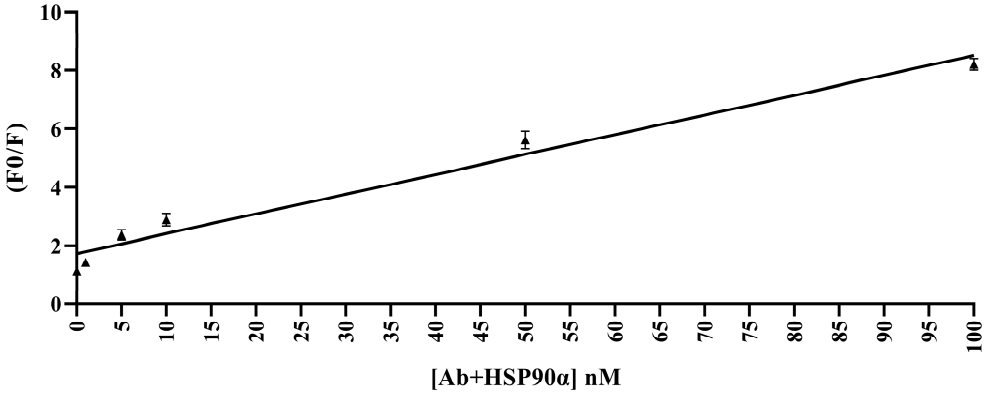

Slope	0.06784
Y-intercept	1.725
R square	0.9702

Figure 6. Masking of Sav-QDs plotted in Stern–Volmer plot as a function of (F0/F) versus HSP90α concentration ranging from 100 to 1 nM. F0 and F are fluorescence intensities of Sav-QDs after adding antibody and HSP90α. K_{SV} is evaluated to be 0.06784 nM^{-1} with linear data regression (r^2 = 0.97). LoD and LoQ of the assay are 5.18 nM (0.45 μg/mL) and 15.2 nM (15.62 μg/mL). These values are nearby the EC_{50} value of biotin-ATP and HSP90α binding assay.

3.4.2. Confirming the Binding of Protein to Biotinylated Antibodies Attached to Sav-QDs

This was done to confirm the binding of the Sav-QD-bound biotin-HSP90 antibody to HSP90α. The fluorescence of the quantum dots was measured in two conditions: the first one was after attachment to the biotinylated antibody, and the second was after HSP90α attachment. An expected increase in the masking of the fluorescence was observed from former to later conditions for 100, 50, and 10 nM concentrations. From 100 to 50 nM, the masking effect decreased for both conditions. From 50 to 10 nM, the masking effect was almost the same for both conditions, indicating its saturation level of masking the given Sav-QD concentration by proteins (Figure 7).

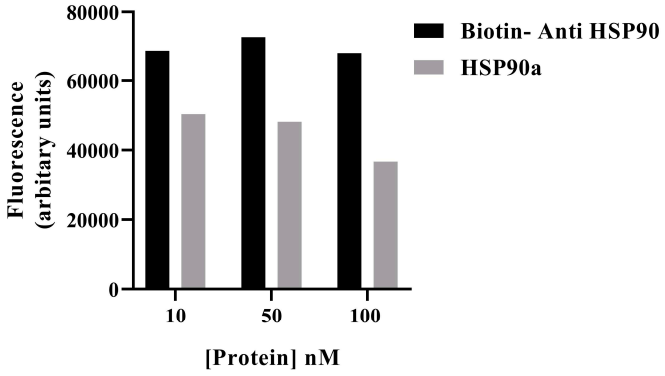

Figure 7. Fluorescence microscopy measurements show a decrease in fluorescence when a comparison was made between the attachment of biotinylated antibodies to Sav-QDs and the attachment of HSP90α to these biotinylated antibodies. Confirming the overall binding of HSP90α to biotinylated antibodies attached to Sav-QDs. The fluorescence signal is plotted against different concentrations of biotin-HSP90α antibody and HSP90α.

3.5. Checking Protein in Cell Lysate

3.5.1. Using Sav-QD Assay to Detect HSP90α in Cell Lysate

It was carried out to detect the presence of HSP90α in HeLa cell lysate and to check if the masking of the fluorescence decreases with dilutions of the cell lysate. The signal difference in each pad between the Sav-QD signal after spotting and after incubation with cell lysate (stock solution, 10× and 100× dilutions) was plotted against antibody and

cell lysate dilutions. The signal difference was chosen because the signal after spotting varied a lot from one pad to another. As the dilution of the cell lysate increases, the signal difference or the masking effect decreases and it is the least for the control (i.e., 1× PBS buffer) (Figure 8). The QD-based assay system is able to detect HSP90α in Hela cell lysate by showing the difference in the HSP90α concentrations.

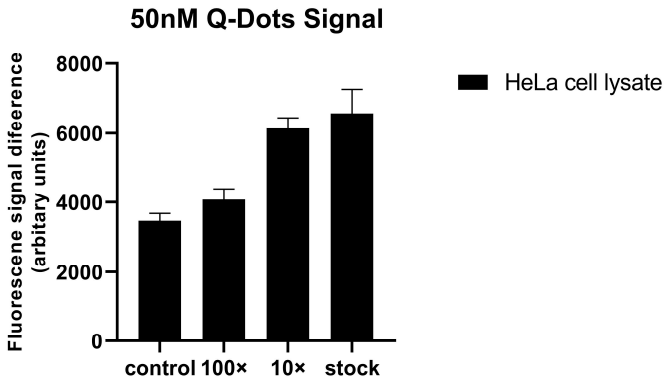

Figure 8. Fluorescence signal difference in Sav-QDs' after spotting and after incubation with biotinylated HSP90 antibody and HeLa cell lysate plotted against different dilutions of HeLa cell lysate. Control is only 1× PBS buffer.

3.5.2. Confirming Presence of HSP90α in Cell Lysate with Western Blot

Western blot was conducted to confirm the HSP90 protein expression in cell lysate. The results of the blotting show that the monomer of HSP90 at around 100 kDa exists in Hela cells, not in the fibroblast lysate, and the enrichment is considerable compared with the purified recombinant HSP90 with an amount of 30 µg. The lysate of 10× and 100× dilution, therefore, were faintly detected of the HSP90 expression. Coomassie-stained SDS-PAGE gel indicates that HSP90 is a predominantly expressed protein in the total lysate proteins of Hela cells (Figure 9).

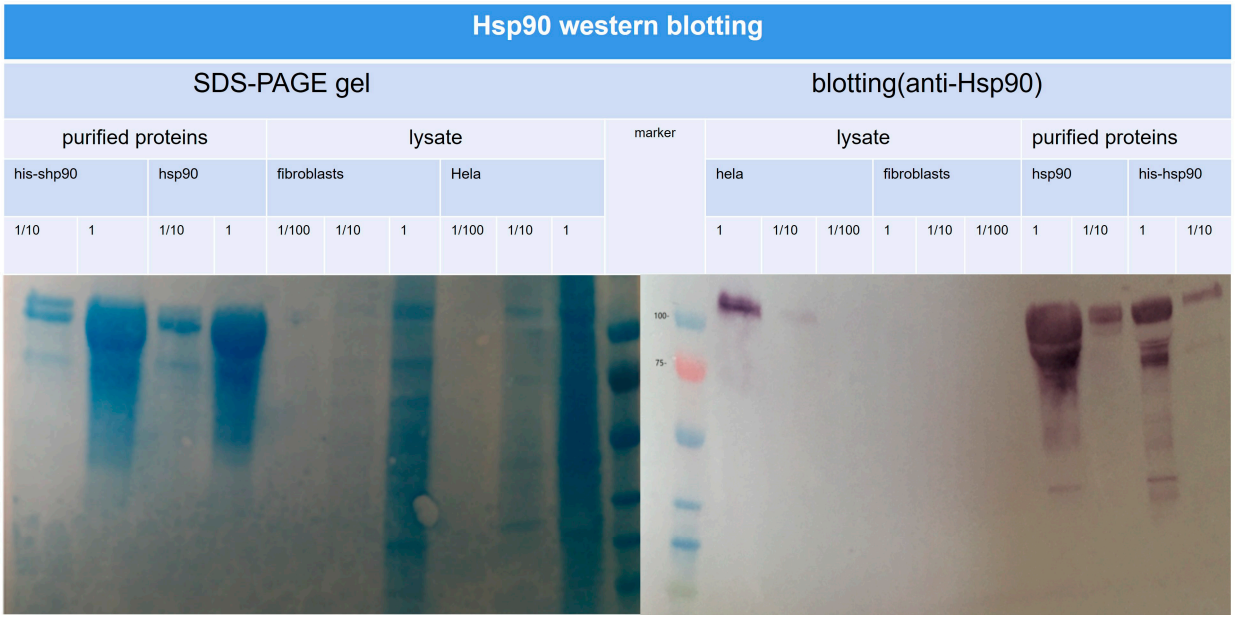

Figure 9. SDS PAGE shows HSP90α is the predominantly expressed protein in HeLa cell lysate compared to other proteins. Western blot confirms the presence of HSP90α in HeLa cell lysate, 10× and 100× dilution around 100 Kd. Negative control fibroblast lysate as negative control has no HSP90α, and positive control is purified HSP90α in stock concentration (30 µg) and 1:10 dilution presents a dose-dependent manner of Hsp90 expression.

3.5.3. Confirming the Binding of HSP90α in Cell Lysate with Biotin-HSP90 Antibody

This was carried out to confirm the binding of the biotin-HSP90 antibody to HSP90α present in HeLa cell lysate. The fluorescence was measured after adding a biotinylated antibody which attached to Sav-QD and after adding cell lysate. There was a decrease in the fluorescence, indicating the masking effect thus confirming the binding of antibody to HSP90α in cell lysate (Figure 10).

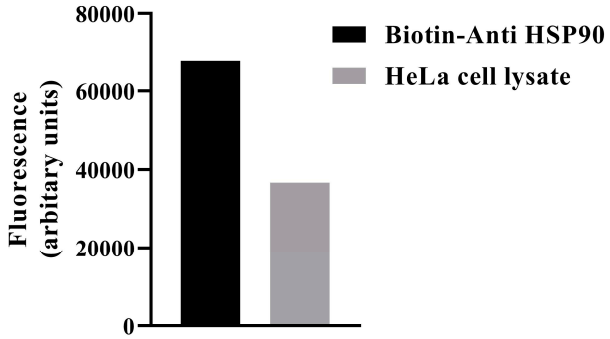

Figure 10. Fluorescence microscopy measurements showed a decrease in fluorescence when a comparison was made between the attachment of biotinylated antibodies to Sav-QDs and the attachment of HSP90α present in HeLa cell lysate to these biotinylated antibodies. Confirming the overall binding of HSP90α present in a complex biological sample such as Hela cell lysate to biotinylated antibodies attached to Sav-QDs. Fluorescence is plotted against samples used for attachment of HSP90α or biotinylated antibodies to Sav-QDs present in PBS buffer.

4. Conclusions

With this technique, we developed a miniaturized and multifunctional assay of Sav-QD for HSP90α detection. Sav-QDs were spotted on the NC surface to measure the fluorescence masking by HSP90α interaction with biotinylated ATP or antibodies, which were attached to Sav-QD through a biotin–streptavidin interaction. It is shown that the binding of the molecules to QDs caused a reduction in the fluorescence. A protein–ligand interaction was observed in a dose-dependent manner using biotin-ATP and HSP90α binding. The inhibitory effect of radicicol was also observed on the binding of ATP and HSP90α; although, a further optimization of the assay is required to remove of the unspecific binding of the proteins and to reveal the complete inhibitory effects of the compounds. In the future, an assay can be further applied to test natural compounds with inhibitory effects for specific protein–ligand interactions. The presence of HSP90α was detected using a protein–protein interaction. Biotinylated antibodies attached to Sav-QDs interacted with HSP90α in a dose-dependent manner, revealing LoD and LoQ in the nano molar range, which was also nearby the EC_{50} value of a biotinylated ATP-HSP90α interaction. This was further applied to detect HSP90α in a complex biological sample such as HeLa cell lysate. An antibody and protein interaction in a purified form and in HeLa cell was confirmed with the fluorescence measurement in the solution and the presence of HSP90α in HeLa cell lysate was confirmed with Western blot. When the traditional assay system was used in a reversed way, i.e., the dye was spotted on the NC surface, and then protein was added for attachment and masking of the signal, it did not work. The reasons could be the unstable attachment of the dye to NC, which was washed away during blocking and incubation with proteins, and the fluorescence of the dye was not high enough for the masking effect to be detected. Tiny volumes in the range of 150 picolitres for one spot were used in this assay; it can be suggested that with 50 μL of QD solution, a large number of microarrays can be prepared. Another advantage is the flexible application of the system as a protein function assay for drug screening and a protein detection assay for antigen presence detection. With optimization, HSP90α can be used as a biomarker for monitoring its presence in blood, oropharyngeal, and nasopharyngeal swabs, providing an invasive, non-invasive, and facile method of sample testing.

In an earlier work, it was found that QDs as dyes in assay format were based on their attachment to the target protein from the top, in which either ligands or proteins were spotted on a solid surface. In this work, we have shown a different approach by spotting the quantum dots on a solid surface by a contactless printing technique. This has miniaturized the assay to a great degree as QDs were spotted in a picolitre volume. The non-contact feature protects the nitrocellulose membrane from being destroyed during printing, thus QDs are attached to it strongly. The single format of the assay is multifunctional as we can detect protein–ligand and protein–protein interactions as well as the effects of inhibitory compounds. With these two features, the assay has the potential to develop into a cheap and compact point-of-care sensor for detecting proteins in multiple ways in biological samples.

Author Contributions: Conceptualization, A.K. and C.Z.; methodology, A.K., L.F., and C.Z.; validation, F.S., C.Z., and T.R.; formal analysis, A.K.; investigation, A.K. and C.Z.; resources, F.S., C.Z., and K.K.; data curation, A.K. and L.F.; writing—original draft preparation, A.K. and L.F.; writing—review and editing, C.Z., K.K., F.S., and T.R.; visualization, A.K., L.F., and C.Z.; supervision, C.Z., K.K. and F.S.; project administration, C.Z. and K.K.; funding acquisition, K.K. All authors have read and agreed to the published version of the manuscript.

Funding: The project was funded by the German Federal Institute of Sport Science (Bundesinstitut für Sportwissenschaft, BISP), project 'Definition of valid and reliable biomarkers including innovative measurement methods for training control in long-distance running' (grant number 070503/20-21.

Institutional Review Board Statement: Not applicable.

Informed Consent Statement: Not applicable.

Data Availability Statement: Raw data available at https://seafile.cloud.uni-hannover.de/d/b650fd2659124575b149/ (accessed on 15 December 2022).

Acknowledgments: We would like to acknowledge Institute of Technical Chemistry, Gottfried-Wilhelm-Leibniz University Hannover for providing infrastructural support and Department of Exercise Physiology and Sports Therapy, Institute of Sports Science, JUSTUS-LIEBIG University, Giessen, Germany, for providing materialistic and financial support.

Conflicts of Interest: The authors declare no conflict of interest. The funders had no role in the design of the study; in the collection, analyses, or interpretation of data; in the writing of the manuscript; or in the decision to publish the results.

References

1. Li, J.; Buchner, J. Structure, function and regulation of the Hsp90 machinery. *Biomed. J.* **2013**, *36*, 106–117. [CrossRef] [PubMed]
2. Wu, T.; Tanguay, R.M. Antibodies against heat shock proteins in environmental stresses and diseases: Friend or foe? *Cell Stress Chaperones.* **2006**, *11*, 1–12. [CrossRef]
3. Kishore, A.; Fetter, A.; Zeilinger, C. Microarray-based screening of putative HSP90 inhibitors predicted and isolated from microorganisms. *Methods Mol. Biol.* **2022**, *2489*, 435–448. [CrossRef] [PubMed]
4. Neckers, L. Hsp90 inhibitors as novel cancer chemotherapeutic agents. *Trends Mol. Med.* **2002**, *8*, S55–S61. [CrossRef] [PubMed]
5. Zubrienė, A.; Gutkowska, M.; Matulienė, J.; Chaleckis, R.; Michailovienė, V.; Voroncova, A.; Venclovas, Č.; Zylicz, A.; Zylicz, M.; Matulis, D. Thermodynamics of radicicol binding to human Hsp90 alpha and beta isoforms. *Biophys. Chem.* **2010**, *152*, 153–163. [CrossRef] [PubMed]
6. Krüger, K.; Reichel, T.; Zeilinger, C. Role of heat shock proteins 70/90 in exercise physiology and exercise immunology and their diagnostic potential in sports. *J. Appl. Physiol.* **2019**, *1*, 916–927. [CrossRef]
7. Takeuchi, T.; Suzuki, M.; Fujikake, N.; Popiel, H.A.; Kikuchi, H.; Futaki, S.; Wada, K.; Nagai, Y. Intercellular chaperone transmission via exosomes contributes to maintenance of protein homeostasis at the organismal level. *Proc. Natl. Acad. Sci. USA* **2015**, *112*, E2497–E2506. [CrossRef] [PubMed]
8. Zhou, V.; Han, S.; Brinker, A.; Klock, H.; Caldwell, J.; Gu, X.-J. A time-resolved fluorescence resonance energy transfer-based HTS assay and a surface plasmon resonance-based binding assay for heat shock protein 90 inhibitors. *Anal. Biochem.* **2004**, *331*, 349–357. [CrossRef]
9. Kwon, O.S.; Hong, T.-J.; Kim, S.K.; Jeong, J.-H.; Hahn, J.-S.; Jang, J. Hsp90-functionalized polypyrrole nanotube FET sensor for anti-cancer agent detection. *Biosens. Bioelectron.* **2010**, *25*, 1307–1312. [CrossRef]

10. Chen, H.; Xue, J.; Zhang, Y.; Zhu, X.; Gao, J.; Yu, B. Comparison of quantum dots immunofluorescence histochemistry and conventional immunohistochemistry for the detection of caveolin-1 and PCNA in the lung cancer tissue microarray. *Mol. Hist.* **2009**, *40*, 261–268. [CrossRef]
11. Goldman, E.R.; Medintz, I.L.; Mattoussi, H. Luminescent quantum dots in immunoassays. *Anal. Bioanal. Chem.* **2006**, *384*, 560–563. [CrossRef] [PubMed]
12. Geho, D.; Lahar, N.; Gurnani, P.; Huebschman, M.; Herrmann, P.; Espina, V.; Shi, A.; Wulfkuhle, J.; Garner, H.; Petricoin, I.E.; et al. Pegylated, Steptavidin-conjugated Quantum dots are effective detection elements for reverse-phase protein microarrays. *Bioconjugate Chem.* **2005**, *16*, 559–566. [CrossRef]
13. Li, M.; Chen, T.; Gooding, J.; Liu, J. Review of Carbon and Graphene Quantum dots for sensing. *ACS Sens.* **2019**, *4*, 1732–1748. [CrossRef]
14. Himmelstoss, S.F.; Hirsch, T. A critical comparison of lanthanide based upconversion nanoparticles to fluorescent proteins, semiconductor quantum dots, and carbon dots for use in optical sensing and imaging. *Methods Appl. Fluoresc.* **2019**, *7*, 022002. [CrossRef] [PubMed]
15. Mattoussi, H.; Mauro, J.M.; Goldman, E.R.; Anderson, G.P.; Sundar, V.C.; Mikulec, F.V.; Bawendi, M.G. Self-assembly of CdSe−ZnS quantum dot bioconjugates using an engineered recombinant protein. *J. Am. Chem. Soc.* **2000**, *122*, 12142–12150. [CrossRef]
16. Goldman, E.; Balighian, E.; Kuno, M.; Labrenz, S.; Anderson, G.; Mauro, J.; Mattoussi, H. Luminescent quantum dot-adaptor protein-antibody conjugates for use in fluoroimmunoassays. *Phys. Stat. Sol.* **2002**, *229*, 407–414. [CrossRef]
17. Lingerfelt, B.M.; Mattoussi, H.; Goldman, E.R.; Mauro, J.M.; Anderson, G.P. Preparation of quantum dot-biotin conjugates and their use in immunochromatography assays. *Anal. Chem.* **2003**, *75*, 4043–4049. [CrossRef] [PubMed]
18. Frasco, F.M.; Chaniotakis, N. Semiconductor quantum dots in chemical sensors and biosensors. *Sensors* **2009**, *9*, 7266–7286. [CrossRef]
19. Goldman, E.R.; Balighian, E.D.; Mattoussi, H.; Kuno, M.K.; Mauro, J.M.; Tran, P.T.; Anderson, G.P. Avidin: A natural bridge for quantum dot-antibody conjugates. *J. Am. Chem. Soc.* **2002**, *124*, 6378–6382. [CrossRef] [PubMed]
20. Yue, Q.; Stahl, F.; Plettenburg, O.; Kirschning, A.; Warnecke, A.; Zeilinger, C. The noncompetitive effect of Gambogic acid displaces fluorescence-labeled ATP but requires ATP for binding to Hsp90/HtpG. *Biochemistry* **2018**, *57*, 2601–2605. [CrossRef]
21. Yüce, M.; Kurt, H. How to make nanobiosensors: Surface modification and characterisation of nanomaterials for biosensing applications. *RSC Adv.* **2017**, *7*, 49386–49403. [CrossRef]
22. Resch-Genger, U.; Grabolle, M.; Cavaliere-Jaricot, S.; Nitschke, R.; Nann, T. Quantum dots versus organic dyes as fluorescent labels. *Nat. Methods* **2008**, *5*, 763–775. [CrossRef] [PubMed]
23. Tran, L.; Park, S. Highly sensitive detection of dengue biomarker using streptavidin-conjugated quantum dots. *Sci. Rep.* **2021**, *11*, 15196. [CrossRef]
24. Arrabito, G.; Pignataro, B. Inkjet printing methodologies for drug screening. *Anal. Chem.* **2010**, *82*, 3104–3107. [CrossRef]
25. Sauer, U. Analytical protein microarrays: Advancements towards clinical applications. *Sensors* **2017**, *17*, 256. [CrossRef] [PubMed]
26. Fan, L.; Kishore, A.; Jansen-Olliges, L.; Wang, D.; Stahl, F.; Psathaki, O.E.; Harre, J.; Warnecke, A.; Weder, J.; Preller, M.; et al. Identification of a Thyroid hormone binding site in Hsp90 with implications for its interaction with Thyroid hormone receptor beta. *ACS Omega* **2022**, *7*, 28932–28945. [CrossRef] [PubMed]
27. Schax, E.; Walter, J.G.; Märzhäuser, H.; Stahl, F.; Scheper, T.; Agard, D.A.; Eichner, S.; Kirschning, A.; Zeilinger, C. Microarray-based screening of heat shock protein inhibitors. *J. Biotechnol.* **2014**, *180*, 1–9. [CrossRef]